

RECONNECTION AT THE HELIOPAUSE

W. Macek

Space Research Centre, Polish Academy of Sciences, Ordona 21, 01-237 Warsaw,
Poland

ABSTRACT

Views of the front side heliopause and different areas, where magnetic field reconnection takes place, are provided for various assumed orientations of the magnetic field of the local interstellar medium. Within these reconnection patches the lines of constant angle between the magnetic field of the unperturbed solar wind (standard Parker's spiral field) and the (uniform) interstellar field, both projected onto the heliopause surface, are computed. Here the shape of the heliopause is described by a simple analytic formula. Explanations of low frequency (2-3 kHz) interplanetary radio emissions detected by Voyager mission and implications of possible observations of the heliospheric boundary are discussed.

INTRODUCTION

Interaction between the solar wind (sw) plasma and the ambient ionized component of the local interstellar medium (LISM) at the heliopause, the boundary separating both media, is considered here, as presented in Figures 1 and 2.

Mixing of plasma due to reconnection processes is a common feature of boundaries of planetary magnetospheres. It is the aim of this paper to show what can heliospheric physics learn from magnetospheric physics in this matter. By analogy with the case of planetary magnetospheres it is argued that field reconnection processes may play an important role for the plasma mixing at the heliopause.

It was first noted by Macek and Grzędzielski that reconnection at the heliopause could provide an important mechanism of plasma transport across the heliospheric boundary /1/. The resulting average rate of the plasma mixing was estimated to be $\sim 10^{-1}$ of the incident mass flow. Moreover, it was suggested that the dependence of the cosmic-ray penetration into the heliosphere on the distribution of these reconnection areas might give some information about the orientation of the LISM magnetic field /1, 2/.

HELIOPAUSE MODEL

Let us consider a simple model of the heliospheric cavity. In Table 1 the total LISM pressure Π^{IS} is taken constant. However, the total solar wind pressure Π^{sw} decreases with the heliocentric distance r as $1/r^2$ (for distant $r \gg r_0 = 1$ AU). Hence, taking the pressure balance one obtains the "nose" of the heliopause to be located at a distance

$$D = r_0 (\Pi^{sw}_0 / \Pi^{IS})^{1/2}. \quad (1)$$

According to equation (1) and using the typical average plasma parameters listed in Table 1 one gets $D \sim 200$ AU. The density profile of the heliospheric cavity corresponding to Table 1 is shown in Figure 1. At the transition region of the heliospheric boundary the plasma density can change due to an inner shock, the heliopause and an outer shock shown in Figure 2 as obtained using hydrodynamic considerations (cf. /3/). The dashed lines in

TABLE 1 Typical Average Plasma Parameters

	Local Inter-Stellar Medium	Solar Wind	
			at $r_0 = 1\text{AU}$ and beyond
Bulk velocity v , km s^{-1}	25	450	$\approx \text{const}$
Ion density n , cm^{-3}	~ 0.04	8	$\propto r^{-2}$
Temperature T , 10^4K	~ 1	10	$\sim \text{const}^*$
Magnetic field B , 10^{-10}T	~ 2	50	$\propto r^{-1} +$

* $\gamma = 1.1-1.2$
 + $B_r \propto r^{-2}$ ($B_r \sim B_\phi$ at 1 AU)

Calculated Pressures (in units of 10^{-12} Pa)

Ram ρv^2	0.042	2711
Thermal $p = 2nkT$	0.011	22
Magnetic $B^2/2\mu_0$	0.016	10
Total Π	0.069	2743

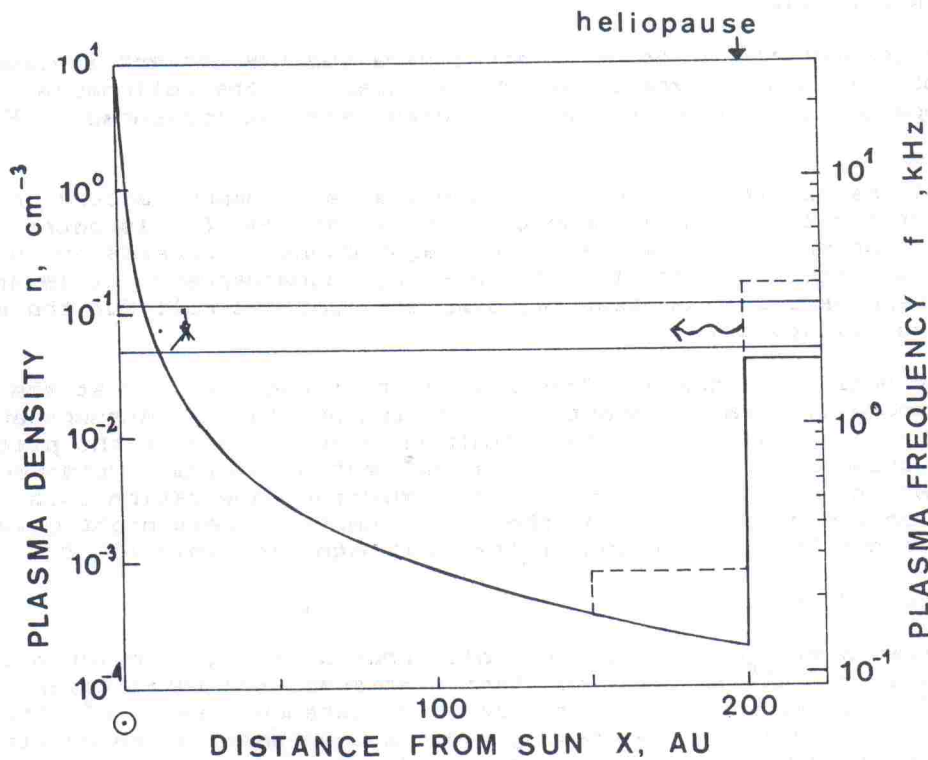


Fig. 1. The density profile of the heliospheric cavity. The heliopause position is indicated. The dashed lines denote only simplified solutions: steps of possible increase of the plasma density by a factor of ≈ 4 due to strongly shocked regions ($\gamma=5/3$, cf./3/). The frequency limits 2 to 3 kHz observed by the plasma wave instruments on Voyager 1 and 2 /6-8/ are also marked.

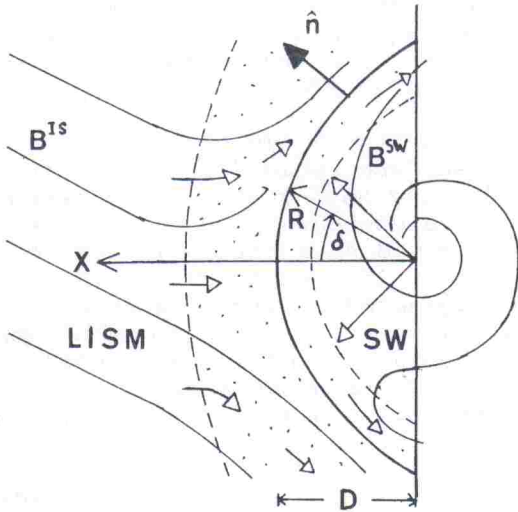


Fig. 2. Sketch of the interfaces between the solar wind (sw) and the supersonic ionized component of the local interstellar medium (LISM: an inner and an outer shocks (dashed) (cf. /3/) and the heliopause of equation (2). Parker's spiral at the inner side and an uniform field at the outer side are taken.

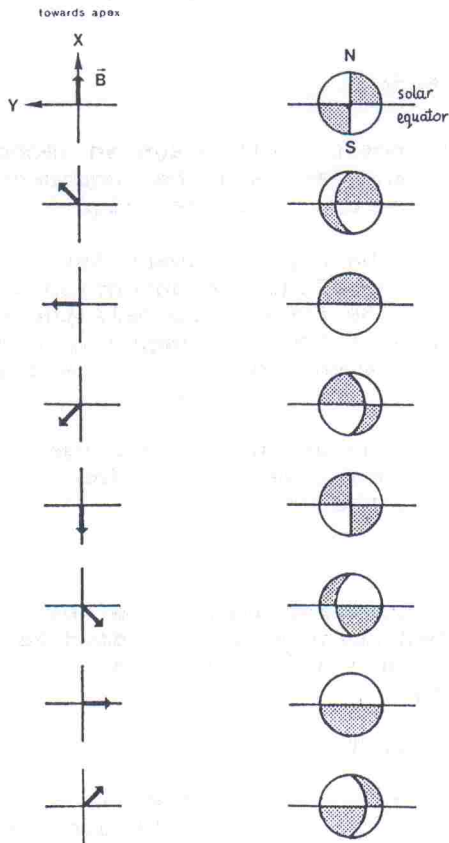


Fig. 3. A view of the heliopause front side shown projected onto the Z-Y plane (X-direction, THETA = 90° PHI = 0°, is collinear with the LISM wind flow vector) depending on the orientation of the interstellar magnetic field vector $B^{IS} = (B^{IS}, \text{THETA}, \text{PHI})$ lying in the solar equatorial (X,Y) plane (taken from /2/).

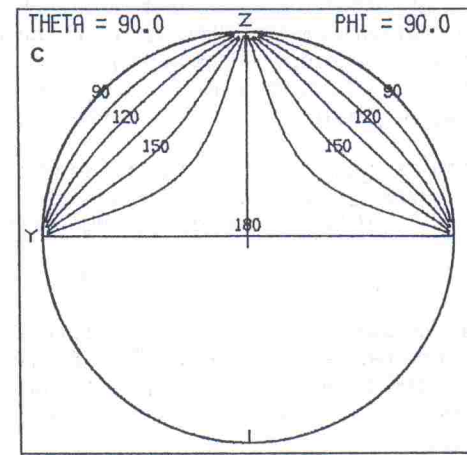
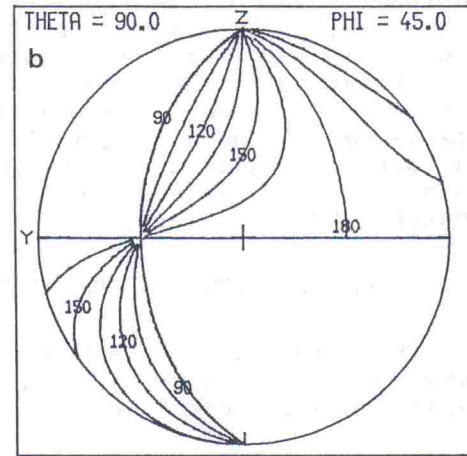
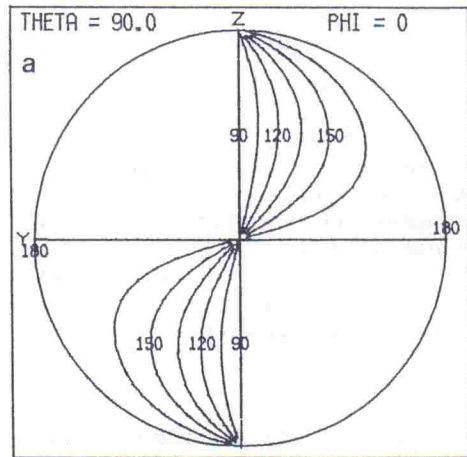


Fig. 4. The lines of constant angle Ψ between the magnetic field H^{SW} of the solar wind and the LISM field H^{IS} , both projected (equations (3)-(4)) onto the heliopause surface given by equation (2), within the reconnection patches: a) for B^{IS} directed towards the apex, and for the direction of B^{IS} changed b) by 45° and c) by 90° from the apex in the solar equatorial (X, Y) plane (SEP).

Figure 1 indicate only simplified solutions: steps of possible increase of the plasma density by a factor of ≈ 4 due to shocked regions ($\gamma=5/3$). The relative thickness of the strongly compressed solar wind region is taken the same as obtained in a hydrodynamic nonmagnetic model of Ref. /3/.

For a standard archimedeian spiral model of the magnetic field of the solar wind one can take $B^{sw} = 1/4 \times 10^{-10}$ T at ~ 200 AU (see Table I in /2/). If the termination solar wind shock is strong B^{sw} could be increased by a factor ≈ 4 . One can expect that both magnetic fields are comparable in magnitudes. Hence, the consideration of the magnetic field should have little influence on the shape of the heliopause (pressure balance). If, additionally, the thermal pressure contribution $p=2nkT$ could be neglected (15% of the total LISM pressure) one can also obtain analytically a more realistic solution for the shape of the heliopause. Namely, one takes only ram pressures on both sides. The LISM flow is assumed to be parallel and the solar wind flow is taken to be radial. Hence, one gets the heliocentric distance $r = R(\delta)$ to the position of the heliopause to be:

$$R / D = \delta / \sin \delta, \quad (2)$$

where δ is the angle measured from the Sun-apex line (X-axis) and the distance D to the nose of the heliopause is given by equation (1). The plasma apex is assumed to be located in the solar equatorial (X,Y) plane (SEP) and is taken to be X-axis ($\theta = 90^\circ$, $\phi = 0^\circ$). Here ϕ (PHI) and θ (THETA) are the equatorial longitude, counted from the apex (X-axis) in the direction of solar rotation, and the equatorial co-latitude counted from the Z-axis of solar rotation, respectively. A deflection of the nose from the apex is not considered here. The solution of equation (2) is shown in Figure 2. It agrees quite well with the numerical results of the hydrodynamic model presented in /3/, where the LISM and the solar wind are treated as unmagnetized media.

RECONNECTION PATTERN AT THE HELIOPAUSE

On the other hand, one can expect that the magnetic field plays an important role whenever both fields have appropriate polarities, and the reconnection processes are most effective when the fields are anti-parallel /1,2/.

We assume that the reconnection takes place if the angle between both fields is greater than 90° . This simplified assumption defines reconnection patches at the heliopause. The view of these areas at the front side heliopause, indicated by dots, depending on the orientation of the LISM magnetic field vector B^{ls} (in the SEP), is shown in Figure 3 (taken from /2/). The observer is thought to be located in the Sun.

Now, the simplest draping consists of a projection of the field lines onto the surface given by equation (2) with a unit normal vector \hat{n} . The direction of the projected line of force is determined by the vector

$$H = \hat{n} \times (B \times \hat{n}). \quad (3)$$

In the present paper, we provide the lines of constant angle Ψ between the projected magnetic field H^{sw} of the unperturbed solar wind (standard Parker's spiral field) and the projected uniform LISM field H^{ls} within the reconnection patches. The angle Ψ is given by

$$H^{ls} \cdot H^{sw} = |H^{ls}| |H^{sw}| \cos \Psi. \quad (4)$$

The lines corresponding to angles Ψ are given in views presented in Figures 4 a, b, and c for B^{ls} lying in the SEP, i.e. for THETA = 90° . The direction of $B^{ls} = (B^{ls}, \text{THETA}, \text{PHI})$ in the frame of reference adopted here is shown in each view. They correspond to the outward polarity of the B^{sw} in the northern solar hemisphere. Views for the LISM field deflected from the SEP by 45° are shown in /4/. The procedure presented in /5/ may be more appropriate for THETA $\sim 0^\circ$ and 180° ("polar caps" of the heliosphere).

The maximum value of the angle Ψ indicates the regions where the reconnection is expected to be most effective. If the direction of the LISM field is changed by 45° and 90° from the direction of the apex in the SEP those regions are shifted from the edge towards the nose of the heliosphere, i.e. the centre of Figures 4 a, b, c.

DISCUSSION

Since 1983 radio emissions in the frequency range of 2 to 3 kHz (marked in Figure 1) were observed by the plasma wave instruments on Voyager 1 and 2 moving in the outer Solar System /6-8/. The detected radio noise was postulated to emanate from the inner shock of the distant solar wind /6/ or from the heliopause itself /2/. Very recently, it has been suggested that the interaction of an anomalous high speed stream with the terminal shock may be responsible for the generation of the most intense emission /9,10/.

Various estimates of the distance to the terminal shock are thoroughly discussed in /9/. The estimate of ~ 135 AU, based on the stream speed inferred from the data /10/ is consistent with the simple picture given in Figure 1, according to Table 1 and equation (1). It is worth to note that the density gradient is expected to be much stronger at the heliopause than at the inner shock front. It indicates that, if the source in question is located at the boundary region of the heliosphere, the *heliopause* rather than the *inner shock front* could be responsible for the generation of these waves shown schematically in Figure 1, as was already suggested in /2/.

It should be noted that the reconnection pattern at the heliopause is expected to be very much sensitive neither to the assumed shape of that boundary surface nor to the model of the draping of the field lines over the heliopause surface /4/. Of course, there is still an open question whether the magnetic fields at the boundary region are sufficiently regular and whether the reconnection between oppositely directed magnetic fields does indeed take place at some regions of the heliopause surface. If so, one should ask: how does reconnection would affect the access of cosmic rays to the Solar System? The answer to these questions could be very important for the interpretation of the measurements of Voyager mission.

ACKNOWLEDGEMENTS

The author is very much indebted to Prof. S. Grzędzielski for illuminating discussions and to Mr. J. Bysiek for helping in numerical calculations of Figure 4, which were performed on the PDP-11/45 computer in the N. Copernicus Astronomical Centre in Warsaw. This research was supported by the Central Program for Fundamental Research under contract O1.20 coordinated by the Space Research Centre of the Polish Academy of Sciences.

REFERENCES

1. W. Macek and S. Grzędzielski, Earth, Jupiter and Sun - similarity of plasma transport across the cavity boundaries, in: *Twenty Years of Plasma Physics*, ed. B. McNamara, Philadelphia, World Scientific, 1985, p. 320.
2. H. J. Fahr, W. Neutsch, S. Grzędzielski, W. Macek, and R. Ratkiewicz-Landowska, *Space Sci. Rev.* **43**, 329 (1986)
3. V. B. Baranov, M. G. Lebedev, and M. S. Ruderman, *Astrophys. Space Sci.* **66**, 441 (1979)
4. W. Macek and J. Bysiek, A model of the reconnection pattern at the heliopause, in ESA SP-285, ed. T. D. Guyenne, Noordwijk, in press (1988)
5. S.-I. Akasofu and D. N. Covey, *Planet. Space Sci.* **29**, 313 (1981)
6. W. S. Kurth, D. A. Gurnett, F. L. Scarf, and R. L. Poynter, *Nature*, **312**, 27 (1984)
7. W. S. Kurth, D. A. Gurnett and F. L. Scarf, *Adv. Space Res.* **6**, 379 (1986)
8. W. S. Kurth, D. A. Gurnett, F. L. Scarf, and R. L. Poynter, *Geophys. Res. Lett.* **14**, 49 (1987)
9. R. L. McNutt, Jr., A solar-wind "trigger" for the outer heliosphere radio emissions and the distance to the terminal shock, *Geophys. Res. Lett.*, in press (1988)
10. R. L. McNutt, Jr., Remote sensing of the termination of the solar wind via in situ plasma measurements, this issue